

Cover Page



Universiteit Leiden



The handle <http://hdl.handle.net/1887/20273> holds various files of this Leiden University dissertation.

Author: Elmalk, Abdalmohsen

Title: Exposing biomolecular properties one molecule at a time

Date: 2012-12-13

Chapter 2

*Dynamic fluorescence photobleaching of single phycobilisome complexes from *Porphyridium cruentum***

* Liu L-N, Elmalk AT, Aartsma TJ, Thomas J-C, Lamers GEM, Zhiu B-C, Zhang Y-Z (2008) Light-Induced Energetic Decoupling as a Mechanism for Phycobilisome-Related Energy Dissipation in Red Algae: A Single Molecule Study. PLoS ONE 3(9): e3134. doi:10.1371/journal.pone.0003134

Summary: *Single molecule spectroscopy is applied to phycobilisomes (PBsomes), the light-harvesting antenna complex in cyanobacteria and red algae. Real-time spectral detection at the single particle level allows us to characterize the dynamic fluorescence behavior of individual phycobilisome in response to intense light. It is revealed that intense green laser light may affect the function of phycoerythrin molecules in intact phycobilisome, thus restricting energy transfer to the PBsome core. In this way, excess energy will be dissipated before photodamage to the reaction center takes place. Our work further indicates that this process is dependent on oxygen. Singlet oxygen is assumed to function at the interaction site between phycoerythins and other phycobilisome components. As a consequence, a novel photoprotective mechanism occurring in phycoerythrin-containing phycobilisomes is proposed. The spectral variety of phycobiliproteins in intact phycobilisome results in not only broader absorption at the visible range, but also in a photoprotective response to excess absorbed energy.*

2.1 Introduction

Phycobilisomes (PBsomes, see Figure 1) are the major light-harvesting antennae complexes in cyanobacteria and red algae. They are capable of absorbing solar light and transfer energy to the chlorophylls (Chls) of photosynthetic reaction centers (RCs) with a high efficiency. PBsomes are supramolecular protein complexes made up of watersoluble phycobiliproteins (PBP) and linker polypeptides¹⁻³. PBP are a distinctively colored group of disk-shaped macromolecular proteins bearing covalently attached open-chain tetrapyrroles, known as phycobilins, orderly assembled into PBsomes. In the absence of photosynthetic RCs, the PBsomes are highly fluorescent. Four spectral groups of PBP are commonly identified: phycoerythrins (PEs), phycoerythrocyanins (PECs), phycocyanins (PCs) and allophycocyanins (APCs). Solar energy is absorbed by the chromophores of PEs ($\lambda_{\max} = 545\text{-}565$ nm) and transferred in turn by nonradiative transfer via PCs ($\lambda_{\max} = 620$ nm), APCs ($\lambda_{\max} = 650$ nm) to the reaction center.

The conventional PBsomes in cyanobacteria have a hemidiscoidal shape, and contain six peripheral rods and a core complex. The peripheral rods are composed of PEs and inner PCs, and three parallel cylinders consisting of APCs form the core of the PBsome complex. Hemiellipsoidal PBsomes in the unicellular red alga *Porphyridium (P.) cruentum* also contain a large number of PE molecules at the peripheral rod endings^{4,5}. In addition to R-phycocyanin (R-PC) and APC, two different spectral types of PEs were found in *P. cruentum*: B-phycocyanin (B-PC) and b-phycocyanin (b-PC)⁶. A specialized type of linker polypeptides, the chromophoric c subunits, are responsible for the association of B-PC molecules in the rod elements, whereas they are absent in b-PCs^{3,7}. The evolution of

PBPs, presumably from APC to PC and to PE, is accompanied by the diversity and increasing number of chromophores ⁸. The spectral diversity of different PBPs within PBsomes is assumed to extend the absorbance range (500–650 nm) of cyanobacteria and red algae, and offers a stepwise transfer of the trapped energy to the RCs. More specifically, the presence of PE in red algae, especially the γ -subunit-containing PE, could broaden the absorbance of red algae which allows increasing light-harvesting capacity.

The large number of chromophores in PBsomes ensures a high light-harvesting yield of photosynthesis. On the other hand, it may be lethal if excess light is absorbed by the PBsomes in relation to the capacity of photosynthetic RCs. In response to excess excitation

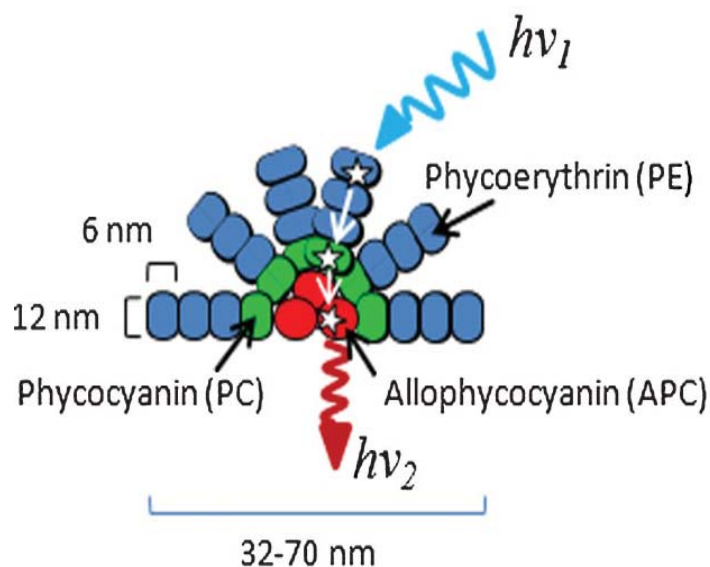


Figure 1: Schematic representation of the three main phycobiliprotein groups in the phycobilisome, the light-harvesting antenna complex in cyanobacteria and red algae. The phycobilisome docks to the membrane-embedded photosynthetic reaction center of the microorganism. The phycobiliproteins, which serve as scaffolding for covalently bound, linear tetrapyrrole chromophores are classified into three types based on their absorption spectra: phycoerythrin (PE), phycocyanin (PC), and allophycocyanin (APC). Hemispherically organized rods of PC and/or PE biliproteins join a core of APC biliproteins. The bulk of the absorption takes place in the rods, while the unique nanostructure facilitates efficient energy transfer towards the core, and from there to the photosynthetic reaction centers.

Phycobiliproteins have strong emission bands that extend well into the red region of the visible spectrum where there is minimal interference from biological materials (e.g. blood, sera and cell culture components). Because of these properties, phycobiliproteins have become promising fluorescent probes for use as a fluorescent marker in immunoassay, flow cytometry, and fluorescence microscopy.

energy, a soluble orange carotenoid protein (OCP) has been demonstrated to be involved in energy dissipation in cyanobacteria⁹⁻¹¹. In contrast, the potential photoprotective response of PBsomes themselves with respect to excess energy is less understood.

The spectroscopy of single molecules or complexes has the great advantage to avoid the ensemble averaging encountered in bulk spectroscopy. Molecular dynamics, for instance molecular conformational changes, energy transfer and photobleaching, can be studied by measuring the real-time fluorescence spectrum at single molecule sensitivity¹². Single-molecule techniques have been extensively applied in photosynthetic systems and provided new insights into the photophysical processes and functional properties of photosynthetic chromophore-protein complexes¹³⁻¹⁸. Effects of photobleaching and interprotein energy transfer of single PBPs have been previously reported, for systems such as B-PE¹⁹, monomers of PEC^{20,21} and APC trimers²². However, spectral properties of intact single PBsome complex are still enigmatic.

Recently a novel approach was explored to monitor single-molecule fluorescence spectra using an Amici prism as a dispersion element^{23,24}. It provides the possibility to investigate real-time fluorescent emission dynamics of PBsomes as well as the energy transfer between various PBsome components. In the present work, we applied single-particle spectroscopy to investigate the PBsomes from *P. cruentum* at room temperature. Green-light-induced photobleaching of single PBsome was demonstrated to involve an energetic decoupling of B-PE within the PBsome rod, serving as a novel pathway of energy dissipation. Our results provide insights into the photobleaching dynamics of PBsomes in red algae, and their photoprotective roles in response to excess light energy.

2.2 Materials and Methods

2.2.1 Sample separation

Porphyridium (P.) cruentum wild-type and mutant F11 strain (UTEX 637) were grown in an artificial sea water medium³⁸. Flasks were supplied with 3% CO₂ in air through a plug of sterile cotton at a constant temperature of 20 °C. Cultures were illuminated continuously with light provided by daylight fluorescent lamps at 6 W.m⁻². The *P. cruentum* F11 mutant was constructed before²⁹ and was shown by LiDS-PAGE³⁰ analyses to be deficient of the c subunit. Intact PBsomes were separated following previously described protocols⁵.

2.2.2 Spectral analysis

Absorbance spectra were recorded with UV-160A spectrophotometer (Shimadzu, Japan). Room-temperature fluorescence spectra were measured with a LS 55 Luminescence

Spectrometer (Perkin-Elmer Instruments, USA). For single-particle experiments, PBsomes were dissolved in 0.75 M phosphate buffer with 1% polyvinyl alcohol (PVA) to a protein concentration of 0.5 $\mu\text{g/ml}$, after which samples were spin-coated on a freshly cleaned microscope cover-glass. For gluteraldehyde (GA) fixation, the dilution buffer contained not only PVA, but also GA with a final concentration of 1% (v/v).

2.2.3 Experimental Setup

The single-molecule fluorescence microscopy setup is based on an Axiovert S100TV inverted microscope with epifluorescent detection. The power density at the sample was 35–1050 $\text{W}\cdot\text{cm}^{-2}$. The light from the laser sources, a Nd:YAG (532 nm) or a solid state laser (639 nm), was passed through a set of optical components (to control intensity and polarization), reflected by a dichroic mirror (transmission centered at 550 nm/660 nm), and focused on the sample by a high numerical aperture water-immersion objective (60 \times , numerical aperture 1.2, Olympus). By inserting an extra lens before the dichroic mirror, which focuses the laser beam at the backplane aperture of the microscope objective, the setup can be switched from a confocal to a wide-field imaging mode. Fluorescence emission from excited molecules was collected with the same objective, filtered after the dichroic mirror with an additional notch filter to reject the remaining scattered laser light and Raman scattered light. For spectral analysis, fluorescence emission was dispersed by an Amici prism and detected with a front-illuminated charge-coupled device (CCD) camera (Cascade 650, Photometrics). The integration time used for the spectral acquisition was 0.3 seconds.

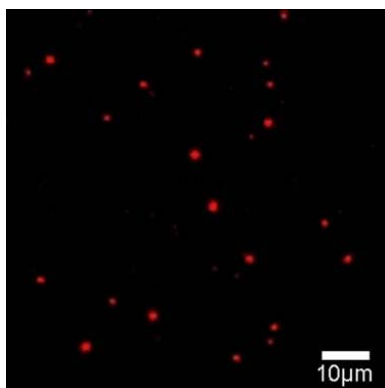


Figure 2. Fluorescence image ($82\times 82 \mu\text{m}^2$) of individual PBsomes at room temperature. Excitation wavelength is 532 nm.

2.3 Results

2.3.1 Fluorescence photobleaching of single PBsomes

Green (532 nm) and red (639 nm) lasers were utilized in this work for high-light illumination. Based on the ensemble absorption spectrum of PBsomes from *P. cruentum*, the 532 nm light is absorbed predominantly by PE, allowing us to investigate the full energy transfer chain within intact PBsomes, from PE to R-PC, then to APC and finally to the PBsome terminal emitters, LCM and α APB²⁵. Figure 2 shows the raw fluorescence image of individual PBsomes excited at 532 nm ($260 \text{ W}\cdot\text{cm}^{-2}$). The complexes were

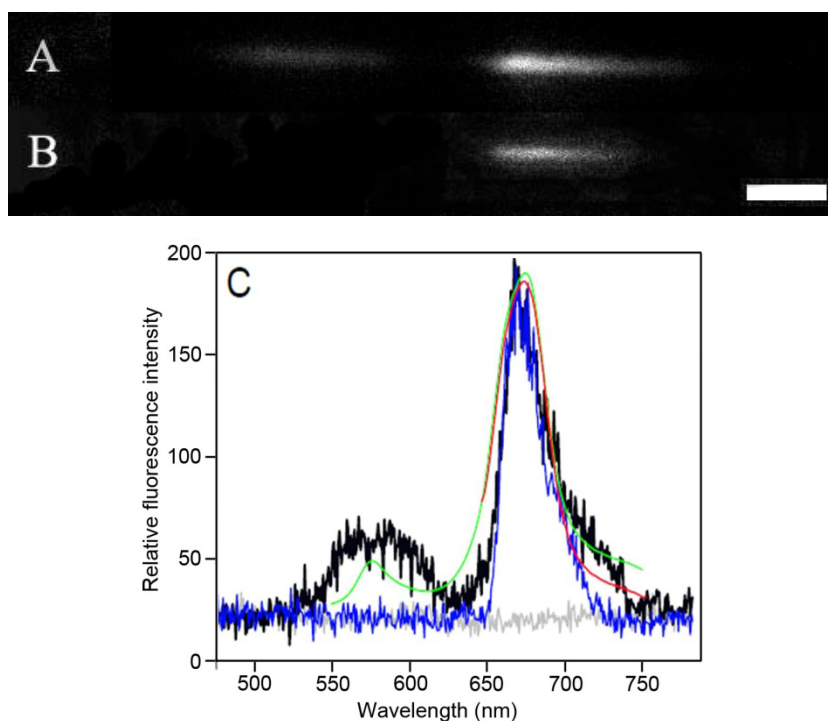


Figure 3. A,B: Fluorescence emission image of single PBsomes at room temperature. Images were obtained in wide-field microscopy combined with dispersion of the epifluorescence by an Amici prism in front of the CCD camera. Single PBsomes were imaged as two bands when excited at 532 nm (A), and a single fluorescence band was recorded when excited at 639 nm (B). C: fluorescence emission spectra of single PBsome excited at 532 nm (black) and 639 nm (blue). The background is shown with light gray. The two emission bands resemble the room-temperature fluorescence ensemble spectra of PBsome in bulk solution (0.75 M phosphate buffer, pH 7.0) when excited at 532 nm (green) and 639 nm (red), respectively.

immobilized on the glass slide by adding 1% (v/v) polyvinyl alcohol (PVA) to a diluted PBsome solution in 0.75 M phosphate buffer, pH 7.0. Due to the high dilution to $0.5 \mu\text{g}\cdot\text{ml}^{-1}$, most of the observed intensity spots represent single PBsomes. A good signal-to-noise ratio of the fluorescence emission was obtained due to the strong fluorescence of PBsome supramolecular complex which carries up to 2000 bilin chromophores, in combination with highly sensitive detection. After dispersion by an Amici prism, two discrete fluorescence bands were recorded simultaneously when a single PBsome was excited at 532 nm (Figure 3A). Full fluorescence emission spectrum of single PBsomes were obtained by integrating the total fluorescence intensities within a selected region on the CCD array and subtracting the background. Figure 3B shows the fluorescence image of a single PBsome when excited at 639 nm. As depicted in Figure 3C, a major fluorescence emission from the PBsome core (674 nm) and a minor fluorescence emission band of PE (576 nm) were observed. We recorded fluorescence spectra of 200 single PBsome complexes acquired with a 400 ms integration time per spectrum. 80% of them (162 single PBsomes) present typical fluorescence of PBsomes. Spectral variation was observed in the other 20% PBsomes, showing decreased fluorescence and a higher ratio of PE/PBsome core fluorescence. It is assumed that the photobleaching of a few PBsomes has taken place under laser illumination in the process of seeking targeting samples. Excitation energy at 639 nm is only absorbed by APC complexes. Therefore, the fluorescence emission of PBsome complex was detected as only a single fluorescence band attributed to the PBsome core (Figures 3B and 3C). These are consistent with the bulk fluorescence spectra (Figure 3C).

We further investigated the fluorescence photobleaching of individual PBsome complexes. As shown in Figure 4A, under illumination with 532 nm laser at $260 \text{ W}\cdot\text{cm}^{-2}$, PBsome core fluorescence exhibited a successive decrease of the fluorescence intensity in combination with a minor blue-shift. This implies that intense green-light induces the photobleaching of the intact PBsome. Surprisingly, PE fluorescence did not present the same photobleaching behavior as the PBsome core fluorescence. Instead, an increase of PE fluorescence intensity at the first seconds of illumination was observed, followed by a decrease. This is clearly evident in the fluorescence intensity traces of two emission bands as a function of time (Figure 4B). It shows a 1.6-fold fluorescence increase of PE emission at the first stage of illumination and a decrease after 50 seconds.

These two distinct stages of PBsome are further revealed by examining the ratio of PE to PBsome core fluorescence. As seen in Figure 4B, the ratio of the fluorescence intensities of PE to PBsome core initially rises drastically above the value of 1.0, due to the combined effects of the increase of PE emission and the rapid decrease of PBsome core emission;

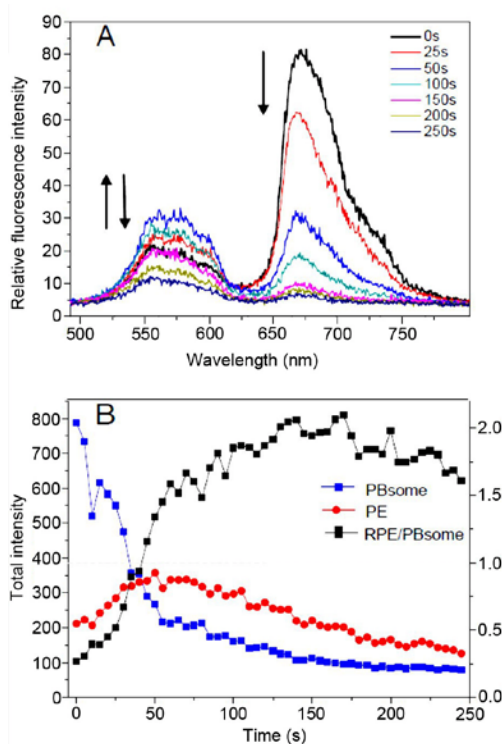


Figure 4. Fluorescence photobleaching of single PBsome under 532 nm illumination at $260 \text{ W}\cdot\text{cm}^{-2}$ during 250 seconds. Integration time is 400 ms. A: fluorescence spectral profiles of single PBsome during photobleaching. Arrows represent the fluorescence changes of PE and PBsome core. B fluorescence intensities of PE (red, 570 nm) and PBsome core (blue, 675 nm) of single PBsome as well as the ratio of fluorescence intensities of PE/PBsome core (black) as a function of time.

afterward it gradually decreases, indicating that at the late stage both emissions are bleached with relatively similar rates. The real-time spectral dispersion thus provides the opportunity to monitor the fluorescence dynamics of PBsome under specific illumination conditions, and to correlate the observations with changes of energy migration. We note that, due to the more complex pigment composition of the PBsomes from *P. cruentum*, the photobleaching profile of single PBsome in this case is different from those of individual PBPs observed before^{19–22}.

2.3.2 Power-dependence of single PBsome fluorescence

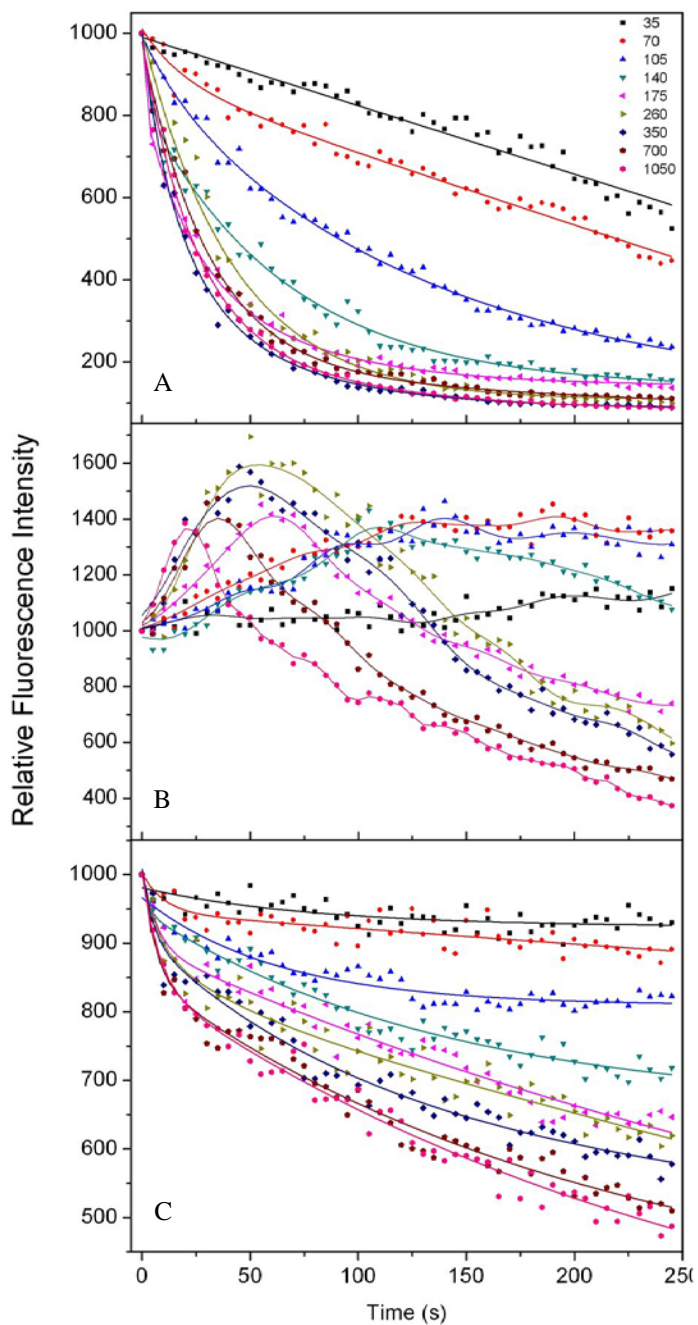
To reveal the effect of illumination power on their fluorescence and photobleaching behavior, single PBsomes were illuminated with a green laser (532nm) at different power

Figure 5. Power-dependence of fluorescence photobleaching of single PBsomes.

A: normalized PBsome fluorescence intensity time courses over the laser power ranging from 35 to $1050 \text{ W}\cdot\text{cm}^{-2}$. Excitation wavelength is 532 nm.

B: normalized PE (570 nm) fluorescence intensity time courses over the laser power range from 35 to $1050 \text{ W}\cdot\text{cm}^{-2}$. Excitation wavelength is 532 nm.

C: normalized PBsome core (675 nm) fluorescence intensity time courses over the laser power range from 35 to $1050 \text{ W}\cdot\text{cm}^{-2}$. Excitation wavelength is 639 nm which can only excite APC.



levels (35 to 1050 $\text{W}\cdot\text{cm}^{-2}$). The light intensity in these experiments is up to a few orders of magnitude higher than under natural conditions. As shown in Figure 5A, the bleaching effect of the individual PBsomes is strongly depending on the laser power up to 140 $\text{W}\cdot\text{cm}^{-2}$. Above 140 $\text{W}\cdot\text{cm}^{-2}$, the photobleaching profiles appeared to be nearly indistinguishable and more than 80% photobleaching was obtained. Figure 5B presents the power dependence of PE emission with excitation at 532 nm. With the increase of laser power, a significant rise of PE emission intensity was observed. The maximum intensity was detected at 260 $\text{W}\cdot\text{cm}^{-2}$. The PE intensity traces reflect competition between an increase of fluorescence intensity and photobleaching. Above 260 $\text{W}\cdot\text{cm}^{-2}$, the photobleaching starts to dominate, limiting the maximal incline of fluorescence intensities. Furthermore, the maximum emission intensity presents a progressive blue-shift with the increase of laser power, indicating that more intense light can result in a faster increase of PE emission. Figure 5C shows the power dependence of PBsome core emission with excitation at 639 nm. Since only APCs can be excited at 639 nm, the power dependent behavior of PBsome core emission may be compared with the PBsome core fluorescence when excited at 532 nm, to provide more insights into energy transfer of intact PBsome.

It was found that the fluorescence of PBsome core complex is unable to be completely bleached (at most up to 50%) in 250 seconds. With absorbance of PBsomes at 532 nm being 6-fold higher than that at 639 nm (see absorption spectrum shown below in section 2.3.4), 1050 $\text{W}\cdot\text{cm}^{-2}$ red laser power is comparable to 175 $\text{W}\cdot\text{cm}^{-2}$ green laser power upon excitation the PBsome complex. 1050 $\text{W}\cdot\text{cm}^{-2}$ red laser induced 50% of photobleaching, whereas 175 $\text{W}\cdot\text{cm}^{-2}$ green laser resulted in as low as 80% of photobleaching, suggesting that the fluorescence loss of PBsome core when excited at 532 nm is composed not only of the photobleaching of PBsome core emission, but also of reduced PE-to-core energy transfer which contributes to the increase of PE emission.

2.3.3 Green laser induces an energetic decoupling of the PBsome

The possibilities for the fluorescence increase of PE are suggested. First, fast energy transfer from PE to the PBsome core allows the PE complexes to be less bleached than PBsome terminal emitters. When down-stream energy acceptors are bleached, excess energy captured by peripheral PE molecules is dissipated from the PE. Another possibility is the decoupling of PE from energy transfer path in the PBsome. Excess energy may increase the rate of bleaching of PE which exists as an isolated individual energy acceptor after the energetic decoupling, and result in further decrease of PE emission. In addition, it is also possible that energy transfer within the PBsomes is much decreased due to the photodamage without physical decoupling of the complex²⁶.

To further reveal the mechanism involved in the fluorescence increase of PE, we investigated single PBsome complex pre-treated with the protein cross-linking agent glutaraldehyde (GA). GA has been commonly used to stabilize PBsome conformations^{5,27,28}. Under the treatment of GA (1%, v/v; 1 min incubation), the PBsome is assumed to remain conformationally and functionally intact. This is corroborated by the fact that bulk (Figure 6A) and single-molecule emission spectra (Figure 6B) before and after GA treatment are identical. Figure 7A shows time courses of the total intensity of PE emission in single PBsome untreated and pre-treated with GA. In contrast to the photobleaching behavior of untreated PBsome, no increase of PE emission was observed after fixation with GA, which indicates that the increase of PE emission observed in the photobleaching of untreated PBsome may be attributed to the energetic decoupling of PE in the PBsome.

In Figure 7B, the photobleaching percentage of PBsome core emission treated with GA is found to be 10% less than that of untreated PBsome. Such a difference is assumed to be attributed to the energetic decoupling of PE molecules. Figure 7C presents the distinct

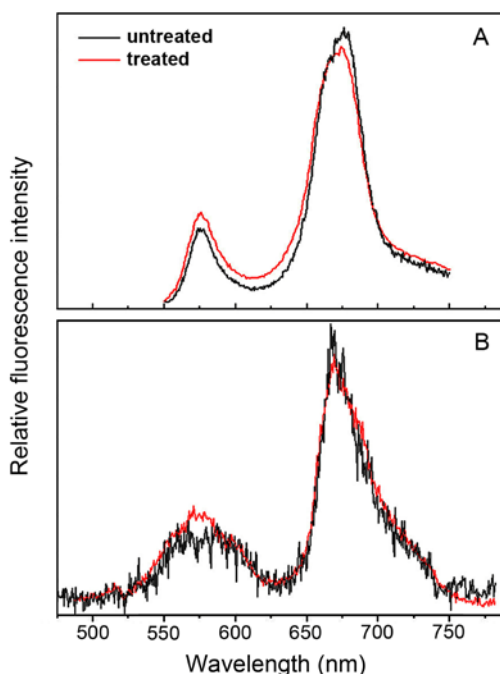


Figure 6. Comparison of the fluorescence properties of PBsomes treated and untreated with glutaraldehyde (GA, 1 min incubation). Excitation wavelength is 532 nm. A: ensemble fluorescence spectra; B: single-molecule fluorescence spectra.

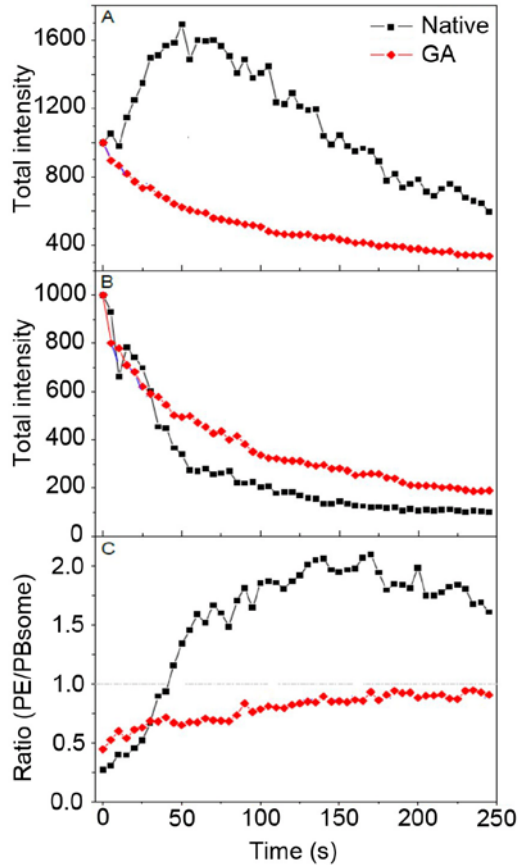


Figure 7. Fluorescence photobleaching of PBsome, native (black) and treated (red) with GA under illumination power of $260 \text{ W}\cdot\text{cm}^{-2}$. A, time course of the photobleaching of PE emission after normalization; B, time course of the photobleaching of PBsome core emission after normalization; C, time course of the ratio of fluorescence intensities of PE/PBsome core.

ratios of PE to PBsome core fluorescence intensity in these two conditions. Untreated PBsome exhibited a drastic incline of the ratio up to the value of 2.0, which suggests that after bleaching PE fluorescence is more pronounced than that of the PBsome core. In contrast, the ratio of fluorescence intensity of the PBsome with GA treatment was observed to be less increased, constantly lower than the value of 1.0. Our data revealed that green-laser-induced energetic decoupling might involve changes of the protein-protein associations within the PBsome.

2.3.4 Fluorescence photobleaching of mutant PBsome

It is noteworthy that the light-induced decoupling of PE in single PBsome can only result in no more than 2 times of fluorescence increase and energy transfer within the complex can still take place. It apparently implies two discrete types of PEs: one group of PEs are involved in the light-induced decoupling, and another group still have a solid association in the PBsome rods to perform energy flow. This is reminiscent of previous observation that two types of PEs, B-PE and b-PE, were found in the rod of *P. cruentum* PBsomes⁶. The distinction between the two is the presence of a c peptide in B-PE but not in b-PE⁷. The mutant strain F11 of *P. cruentum* was characterized to contain a lower level of PE content in light of the complete deficiency of c subunits, the B-PE-associated chromophoric linker polypeptides, revealed by LiDS-PAGE (lithium dodecyl sulfate polyacrylamide gel electrophoresis) experiments^{29,30}. Absorption spectra of ensemble PBsomes from wild-type (WT) and F11 *P. cruentum* show that one third of PE is retained in the mutant PBsome compared to WT PBsome (Figure 8A). It is most likely that the remaining are b-PE molecules which assemble with neighboring R-PC by linker polypeptides which are different from the c subunits. The smaller dimension of mutant PBsome because of a reduced PE content is also confirmed by our TEM results (data not shown).

As a comparative investigation, we examined the fluorescence emission properties of single PBsome prepared from mutant F11. In terms of the reduced absorbance at 532 nm in this mutant, a laser intensity of $700 \text{ W}\cdot\text{cm}^{-2}$ was applied on the F11 PBsome compared to $260 \text{ W}\cdot\text{cm}^{-2}$ on WT PBsome in order to obtain identical excitation conditions. Figure 8B shows a dispersed fluorescence emission of single PBsome from F11 excited at 532 nm green laser. Two separated fluorescence bands are detected, reminiscent of the fluorescence property of the WT PBsome. In addition to the identical emission positions, we found that the PE fluorescence of mutant PBsome is weaker than that of WT PBsome, which probably suggests a higher efficiency of energy transfer in mutant PBsome (Figure 8C). It may imply the flexible assembly between B-PE and b-PE in WT PBsomes, as well as the relatively solid interaction between b-PE and neighboring R-PC hexamer. During the process of photobleaching, both PE and PBsome core emissions of F11 PBsome are quenched in parallel (Figure 8D). The intensity ratios of b-PE to PBsome core fluorescence are relatively constant, lower than the value of 1.0. Unlike WT PBsomes, the increase of PE emission intensity during the bleaching was not seen, suggesting that B-PE molecules which are located at the peripheral side of WT PBsome rods are predominately responsible for the energetic decoupling of PBsome, whereas b-PE is probably not involved.

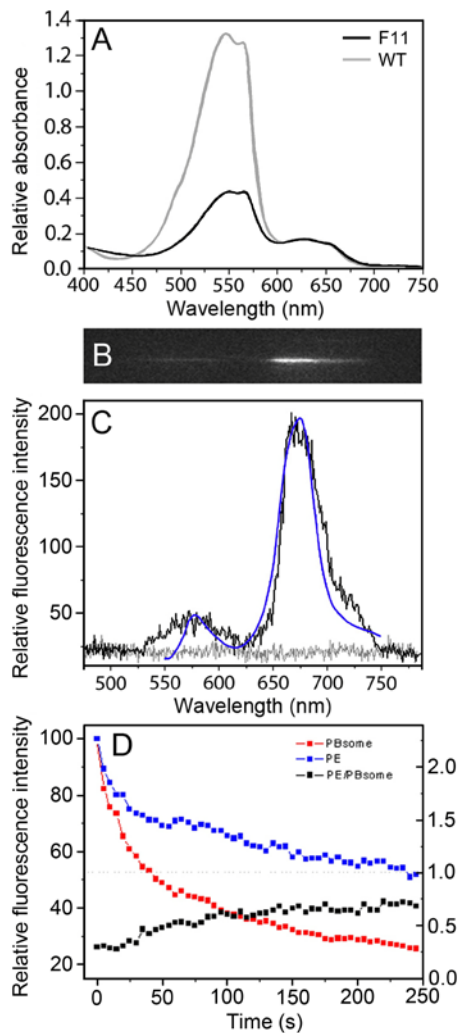


Figure 8. Single-molecule properties of PBsome from mutant *P. cruentum* F11. A, absorbance of ensemble PBsome from WT and mutant strain. A532 of F11 PBS is as low as 35% than WT PBsome, so laser power performed on F11 PBsome is 700 $\text{W}\cdot\text{cm}^{-2}$. B, fluorescence emission image of single F11 PBsome at room temperature obtained in wide-field microscopy dispersed by the Amici prism front of CCD camera. C, single PBsome was imaged as two fluorescence bands when excited at 532 nm (black). Background is presented with light gray. Room-temperature fluorescence emission spectra of isolated mutant PBsome (0.75 M phosphate buffer, pH 7.0) were recorded when excited at 532 nm (blue). D, total intensities of PE (■) and PBsome core (■) emission of single PBsome as well as their ratio (■) as a function of time.

2.4 Discussion and Conclusions

The strong fluorescence of the PBsomes, due to the abundance of chromophores carried in the PBsomes, is shown to be an advantage for the sensitive detection of individual complexes. We applied fluorescence detection at the single-molecule level to investigate, for the first time, the fluorescence of the PBsomes in *P. cruentum* dispersed through an Amici prism. The real-time fluorescence detection is able to reveal the spectral dynamics and energy transfer of the chromophore-protein complexes. The results allow us to better characterize the effects of intense light on the PBsomes. It is demonstrated that strong green-light can induce the photobleaching of the PBsomes, as shown by the drastic decline of PBsome core fluorescence. More importantly, a great proportion of excitation energy, surprisingly, is found to be dissipated in the form of PE fluorescence. Our comparative results, which show that such an increase is absent in the photobleaching of GA-treated PBsome, verified the green-light-induced energetic decoupling of PE in the PBsome. The PBsome rods in cyanobacteria comprise in general one or up to two types of PBPs, whereas those in red alga *P. cruentum* contain in turn B-PE that carries c-subunit, b-PE that does not carry a γ -subunit, and R-PC from the periphery to the interior of the rod. Therefore, the PBsomes of *P. cruentum* is an ideal model to study the energy transfer pathway. The different behaviors of PE fluorescence in WT and mutant experiments presented in this work strongly indicate the distinct contributions of B-PE and b-PE in the energy transfer of PBsomes.

On the basis of our observations, a schematic model of light induced energetic decoupling of PBsome was proposed, as depicted in Figure 9. It is characterized that B-PE and b-PE are coupled face-to-face at the periphery of PBsome rod. The outer B-PE presents potentially a flexible energetic association with the inner b-PE with the assistance of the c subunit of B-PE. The photobleaching of PBsome is accompanied by the energetic decoupling which preferentially occurs in the b-PE - B-PE interaction site. It is presumably that the c subunits, the specific linker polypeptides which carry phycobilins, might play an important role in the energetic decoupling of PBsomes in *P. cruentum*. On the other hand, assuming that the same process occurs also at the much lower physiological light intensities, our observations have important implications on the photoprotection function of PBsomes. So far, the mechanism of the antenna-related photoprotection of OCP in cyanobacteria has been elucidated⁹⁻¹¹. The general concept is that PBsome can not dissipate excess absorbed energy without assistance³¹⁻³³. Such an energetic decoupling of PBsomes with respect to intense light may presumably allow excess photon energy from PE to photosynthetic RCs to be modulated to minimize the risk of chlorophyll photooxidation. This is corroborated with the findings about high-light-induced

reorganization³⁴ and photodegradation of PBsome³⁵. The light-induced conformational altering of PBsome was also found in UV-treated PBsome from which a PE fluorescence increase has been observed, arising from the disassembly of PBsome components³⁶. The photoprotection role of PE in the PBsomes of cyanobacteria on dissipating excess light energy to prevent the photodamage of RCs has been previously interpreted³⁷. Here, despite the high involvement of PE in the light-induced energetic decoupling of PBsomes, we further found specifically that the different roles of BPE that carries chromophoric γ -subunit and b-PE that lacks c subunit in the photoprotective mechanism of red algae. In addition to the roles in PBPs assembly and energy migration, the chromophoric γ -subunit is preferentially sensitive to the intense light, and probably functions in the photoprotection of PBsome. As a primitive unicellular red alga, *P. cruentum* contains the specific γ -subunits and colorless linker polypeptides to assemble B-PE and b-PE hexamer complexes, respectively, in the PBsome rods. The evolution of cyanobacteria and red algae is revealed to be accompanied by the evolution of PBPs⁸. The chromophore variety and increasing number extend the absorbance spectrum and enhance the absorption capacity, enabling the photosynthetic organisms to survive in various environments. Furthermore, our data provide new insights into the biological roles of the chromophore variety: the spectral variety of PBPs in intact PBsomes and the appearance of chromophoric γ -subunit may generate a multi-step photoprotection to effectively prevent photodamage of photosynthetic RCs in response to excess excitation energy *in vivo*.

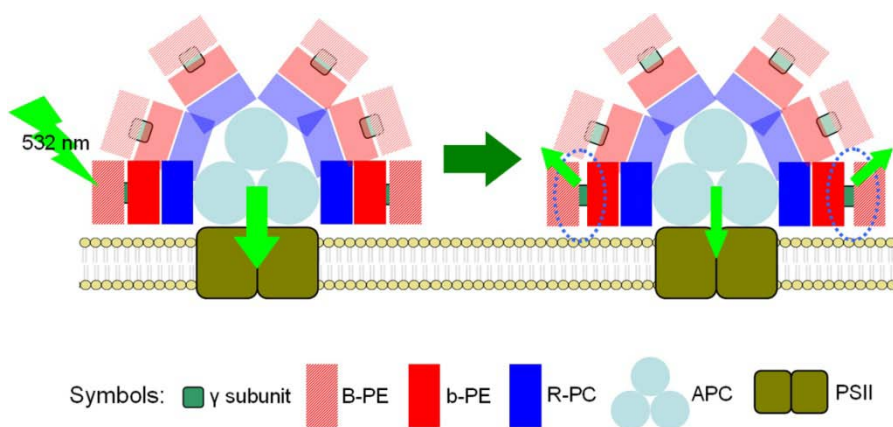


Figure 9. Schematic model of light-induced energetic decoupling of PBsomes. Arrows represent the fluorescence emissions from PBsome components during photobleaching. Dashed circles present the proposed decoupling sites within the PBsome.

References

1. MacColl R (1998) Cyanobacterial phycobilisomes. *J Struct Biol* 124: 311–334.
2. Adir N (2005) Elucidation of the molecular structures of components of the phycobilisome: reconstructing a giant. *Photosynth Res* 85: 15–32.
3. Liu LN, Chen XL, Zhang YZ, Zhou BC (2005) Characterization, structure and function of linker polypeptides in phycobilisomes of cyanobacteria and red algae: an overview. *Biochim Biophys Acta* 1708: 133–142.
4. Gantt E, Lipschultz CA, Zilinskas B (1976) Further evidence for a phycobilisome model from selective dissociation, fluorescence emission, immunoprecipitation, and electron microscopy. *Biochim Biophys Acta* 430: 375–388.
5. Arteni AA, Liu LN, Aartsma TJ, Zhang YZ, Zhou BC, et al. (2008) Structure and organization of phycobilisomes on membranes of the red alga *Porphyridium cruentum*. *Photosynth Res* 95: 169–174.
6. Gantt E, Lipschultz CA (1974) Phycobilisomes of *Porphyridium cruentum*: pigment analysis. *Biochemistry* 13: 2960–2966.
7. Ficner R, Huber R (1993) Refined crystal structure of phycoerythrin from *Porphyridium cruentum* at 0.23-nm resolution and localization of the gamma subunit. *Eur J Biochem* 218: 103–106.
8. Apt KE, Collier JL, Grossman AR (1995) Evolution of the phycobilliproteins. *J Mol Biol* 248: 79–96.
9. Kirilovsky D (2007) Photoprotection in cyanobacteria: the orange carotenoid protein (OCP)-related non-photochemical-quenching mechanism. *Photosynth Res* 93: 7–16.
10. Wilson A, Boulay C, Wilde A, Kerfeld CA, Kirilovsky D (2007) Light-induced energy dissipation in iron-starved cyanobacteria: roles of OCP and IsiA proteins. *Plant Cell* 19: 656–672.
11. Wilson A, Ajlani G, Verbatz JM, Vass I, Kerfeld CA, et al. (2006) A soluble carotenoid protein involved in phycobilisome-related energy dissipation in cyanobacteria. *Plant Cell* 18: 992–1007.
12. Luong AK, Gradinaru CC, Chandler DW, Hayden CC (2005) Simultaneous time- and wavelength-resolved fluorescence microscopy of single molecules. *J Phys Chem B* 109: 15691–15698.
13. Bopp MA, Jia Y, Li L, Cogdell RJ, Hochstrasser RM (1997) Fluorescence and photobleaching dynamics of single light-harvesting complexes. *Proc Natl Acad Sci U S A* 94: 10630–10635.
14. Bopp MA, Sytnik A, Howard TD, Cogdell RJ, Hochstrasser RM (1999) The dynamics of structural deformations of immobilized single light-harvesting complexes. *Proc Natl Acad Sci U S A* 96: 11271–11276.
15. Hofmann C, Ketelaars M, Matsushita M, Michel H, Aartsma TJ, et al. (2003) Single-molecule study of the electronic couplings in a circular array of molecules: light-harvesting-2 complex from *Rhodospirillum rubrum*. *Phys Rev Lett* 90: 013004.
16. Hofmann C, Aartsma TJ, Michel H, Kohler J (2003) Direct observation of tiers in the energy landscape of a chromoprotein: a single-molecule study. *Proc Natl Acad Sci U S A* 100: 15534–15538.
17. Vacha F, Bumba L, Kaftan D, Vacha M (2005) Microscopy and single molecule detection in photosynthesis. *Micron* 36: 483–502.

18. van Oijen AM, Ketelaars M, Kohler J, Aartsma TJ, Schmidt J (1999) Unraveling the electronic structure of individual photosynthetic pigment-protein complexes. *Science* 285: 400–402.
19. Wu M, Goodwin PM, Ambrose WP, Keller RA (1996) Photochemistry and fluorescence emission dynamics of single molecules in solution: B-phycoerythrin. *J Phys Chem* 100: 17406–17409.
20. Zehetmayer P, Hellner T, Parbel A, Scheer H, Zumbusch A (2002) Spectroscopy of single phycoerythrocyanin monomers: dark state identification and observation of energy transfer heterogeneities. *Biophys J* 83: 407–415.
21. Zehetmayer P, Kupka M, Scheer H, Zumbusch A (2004) Energy transfer in monomeric phycoerythrocyanin. *Biochim Biophys Acta* 1608: 35–44.
22. Ying L, Xie XS (1998) Fluorescence spectroscopy, exciton dynamics, and photochemistry of single allophycocyanin trimers. *J Phys Chem B* 102: 10399–10409.
23. Mackowski S, Woermke S, Brotsudarmo TH, Jung C, Hiller RG, et al. (2007) Energy transfer in reconstituted peridinin-chlorophyll-protein complex: ensemble and single molecule spectroscopy studies. *Biophys J* 93: 3249–3258.
24. Wormke S, Mackowski S, Brotsudarmo THP, Brauchle C, Garcia A, et al. (2007) Detection of single biomolecule fluorescence excited through energy transfer: Application to light-harvesting complexes. *Appl Phys Lett* 90: 193901–193903.
25. Glazer AN (1984) Phycobilisome. A macromolecular complex optimized for light energy transfer. *Biochim Biophys Acta* 768: 29–51.
26. Lao K, Glazer AN (1996) Ultraviolet-B photodestruction of a light-harvesting complex. *Proc Natl Acad Sci U S A* 93: 5258–5263.
27. Gantt E, Lipschultz CA (1972) Phycobilisomes of *Porphyridium cruentum*. I. Isolation. *J Cell Biol* 54: 313–324.
28. Biggins J, Campbell CL, Bruce D (1984) Mechanism of the light state transition in photosynthesis. 2. Analysis of phosphorylated polypeptides in the red alga, *Porphyridium cruentum*. *Biochim Biophys Acta* 767: 138–144.
29. Sivan A, Arad SM (1993) Induction and characterization of pigment mutants in the red microalga *Porphyridium* sp (Rhodophyceae). *Phycologia* 32: 68–72.
30. Sivan A, Thomas JC, Dubacq JP, Moppes D, Arad S (1995) Protoplast fusion and genetic complementation of pigment mutations in the red microalga *Porphyridium* sp. *J Phycol* 31: 167–172.
31. Suter GW, Mazzola P, Wendler J, Holzwarth AR (1984) Fluorescence decay kinetics in phycobilisomes isolated from the bluegreen alga *Synechococcus* 6301. *Biochim Biophys Acta - Bioenergetics* 766: 269–276.
32. Rakhimberdieva MG, Stadnichuk IN, Elanskaya IV, Karapetyan NV (2004) Carotenoid-induced quenching of the phycobilisome fluorescence in photosystem II-deficient mutant of *Synechocystis* sp. *FEBS Lett* 574: 85–88.
33. Rakhimberdieva MG, Bolychevtseva YV, Elanskaya IV, Karapetyan NV (2007) Protein-protein interactions in carotenoid triggered quenching of phycobilisome fluorescence in *Synechocystis* sp. PCC 6803. *FEBS Lett* 581: 2429–2433.

34. Stoitchkova K, Zsiros O, Javorfi T, Pali T, Andreeva A, et al. (2007) Heat- and light-induced reorganizations in the phycobilisome antenna of *Synechocystis* sp. PCC 6803. Thermo-optic effect. *Biochim Biophys Acta* 1767: 750–756.
35. Rinalducci S, Pedersen JZ, Zolla L (2008) Generation of reactive oxygen species upon strong visible light irradiation of isolated phycobilisomes from *Synechocystis* PCC 6803. *Biochim Biophys Acta* 1777: 417–424.
36. Six C, Joubin L, Partensky F, Holtzendorff J, Garczarek L (2007) UV-induced phycobilisome dismantling in the marine picocyanobacterium *Synechococcus* sp. WH8102. *Photosynth Res* 92: 77–86.
37. Wyman M, Gregory RP, Carr NG (1985) Novel role for phycoerythrin in a marine cyanobacterium, *Synechococcus* strain DC2. *Science* 230: 818–820.
38. Jones RF, Speer HL, Kury W (1963) Studies on the growth of the red alga *Porphyridium cruentum*. *Physiol Plant* 16: 636–643.

